J|A|C|S
A R T I C L E S

Protonation of Gas-Phase Aromatic Molecules: IR Spectrum of the Fluoronium Isomer of Protonated Fluorobenzene

Nicola Solcà and Otto Dopfer*

Contribution from the Institut für Physikalische Chemie, Universität Basel, Klingelbergstrasse 80, CH-4056 Basel, Switzerland

Received July 30, 2002; Revised Manuscript Received November 12, 2002; E-mail: otto.dopfer@unibas.ch

Abstract: The IR spectrum of the fluoronium isomer of protonated fluorobenzene (F-$C_6H_6F^+$, phenylfluoronium) is recorded in the vicinity of the C−H and F−H stretch fundamentals to obtain the first structured spectrum of an isolated protonated aromatic molecule in the gas phase. Stable F-$C_6H_6F^+$ ions are produced via proton transfer from CH_5^+ to fluorobenzene (C_6H_5F) in a supersonic plasma expansion. The F-$C_6H_6F^+$ spectrum recorded between 2540 and 4050 cm^{-1} is consistent with a weakly bound ion−dipole complex composed of HF and the phenyl cation, HF−$C_6H_5^+$. The strongest transition occurs at 3645 cm^{-1} and is assigned to the F−H stretch (σ_{FH}). The antisymmetric C−H stretch of the two ortho hydrogen atoms, σ_{CH} = 3125 cm^{-1}, is nearly unshifted from bare $C_6H_5^+$, indicating that HF complexation has little influence on the C−H bond strength of $C_6H_5^+$. Despite the simultaneous production of the more stable ring protonated carbenium isomers of $C_6H_6F^+$ (fluorobenzenium) in the electron ionization source, F-$C_6H_6F^+$ can selectively be photodissociated into $C_6H_5^+$ and HF under the present experimental conditions, because it has a much lower dissociation energy than all carbenium isomers. Quantum chemical calculations at the B3LYP and MP2 levels of theory using the 6-311G(2df,2pd) basis support the interpretation of the experimental data and provide further details on structural, energetic, and vibrational properties of F-$C_6H_6F^+$, the carbenium isomers of $C_6H_6F^+$, and other weakly bound HF−$C_6H_5^+$ ion−dipole complexes. The dissociation energy of F-$C_6H_6F^+$ with respect to dehydrofluorination is calculated as D_0 = 4521 cm^{-1} (∼54 kJ/mol). Analysis of the charge distribution in F-$C_6H_6F^+$ supports the notation of a HF−$C_6H_5^+$ ion−dipole complex, with nearly the whole positive charge of the added proton distributed over the $C_6H_5^+$ ring. As a result, protonation at the F atom strongly destabilizes the C−F bond in C_6H_5F.

1. Introduction

Protonation of aromatic molecules is a process of fundamental relevance in chemical and biological disciplines. Protonated aromatic molecules (denoted AH^+) appear frequently as reactive intermediates in (bio)chemical reactions.[1,2] Thus, the characterization of AH^+ is of major interest to understand and possibly control the dynamics and selectivity of chemical processes. For example, AH^+ are widely accepted as short-lived intermediates in electrophilic aromatic substitution reactions, one of the most characteristic reaction mechanisms of aromatic molecules. They occur as σ-complexes (Wheland intermediates) or as π-complexes.[1,2] In the past, NMR and IR spectroscopy were extensively employed to characterize AH^+ ions in the condensed phase.[3−6] Under solvation conditions, however, intrinsic properties of AH^+ are difficult to elucidate, because of the strong

interaction with the environment, such as surrounding solvent molecules and negative counterions.

To separate solvent and matrix effects from molecular electronic properties, gas-phase studies of AH^+ are required.[7−9] To date, nearly all structural and energetic information about isolated AH^+ ions has come from mass spectrometry.[7−9] These techniques provide, however, limited and often indirect structural information (in particular, about the site of protonation), because the interpretation of the experimental data is frequently disputable.[9−11] On the other hand, spectroscopic techniques (especially IR spectroscopy) are sensitive tools to unambiguously derive the structure of molecules. However, a spectroscopic determination of the geometry of any isolated AH^+ ion has not been reported so far, probably due to the difficulties encountered in the generation of sufficient ion densities.[12] Recently, gas-phase IR spectra of weakly bound clusters of protonated benzene ($C_6H_7^+$) and protonated phenol ($C_6H_7O^+$) provided the first spectroscopic characterization of small AH^+

(1) Carey, F. A.; Sundberg, R. J. *Advanced Organic Chemistry*; Plenum Press: New York, 1995.
(2) March, J. *Advanced Organic Chemistry: Reactions, Mechanisms, and Structure*; Wiley: New York, 1992.
(3) Olah, G. A.; White, A. M.; O'Brien, D. H. *Chem. Rev.* **1970**, *70*, 561.
(4) Perkampus, H. H.; Baumgarten, E. *Angew. Chem., Int. Ed. Engl.* **1964**, *3*, 776.
(5) Koptyug, V. A. *Top. Curr. Chem.* **1984**, *122*, 1.
(6) Brouwer, D. M.; Mackor, E. L.; MacLean, C. Arenonium Ions. In *Carbonium Ions*; Olah, G. A., Schleyer, P. v. R., Eds.; Wiley: New York, 1970; Vol. II.

(7) Fornarini, S. *Mass Spectrom. Rev.* **1997**, *15*, 365.
(8) Fornarini, S.; Crestoni, M. E. *Acc. Chem. Res.* **1998**, *31*, 827.
(9) Kuck, D. *Mass Spectrom. Rev.* **1990**, *9*, 583.
(10) Mason, R. S.; Williams, C. M.; Anderson, P. D. J. *J. Chem. Soc., Chem. Commun.* **1995**, 1027.
(11) Solcà, N.; Dopfer, O. *Angew. Chem., Int. Ed.* **2002**, *41*, 3628.
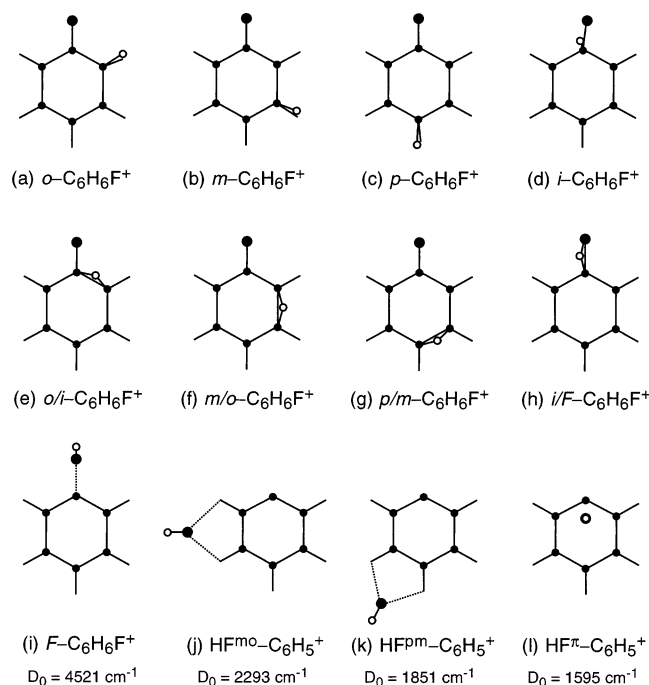(12) Bieske, E. J.; Dopfer, O. *Chem. Rev.* **2000**, *100*, 3963.

Figure 1. Sketch of various structures on the PES of $C_6H_6F^+$ calculated at the B3LYP/6-311G(2df,2pd) level. C and F atoms of C_6H_5F are represented by ●, and the added proton is represented by ○. Protonation may occur at the aromatic ring in the ortho (o-$C_6H_6F^+$), meta (m-$C_6H_6F^+$), para (p-$C_6H_6F^+$), and ipso (i-$C_6H_6F^+$) positions to form stable carbenium ions (fluorobenzenium, a−d). Transition states for proton migration from x-$C_6H_6F^+$ toward y-$C_6H_6F^+$ are denoted x/y-$C_6H_6F^+$ (e−h). The fluoronium isomer (F-$C_6H_6F^+$, phenylfluoronium) and other minima on the PES of the HF−$C_6H_5^+$ ion−dipole complex are shown in (i−l) along with their calculated dissociation energies.

ions under controlled solvation conditions.[11,13] In these studies, the sensitive technique of IR photodissociation (IRPD) spectroscopy was employed to overcome the problems arising from low ion concentrations. IR spectra of $C_6H_7^+$−L and $C_6H_7O^+$−L_n were obtained by monitoring the evaporation of weakly bound inert ligands (L = Ar, N_2) via resonant vibrational predissociation. This approach utilizes L as a "messenger",[12,14] because the perturbation of $C_6H_7^+$ and $C_6H_7O^+$ by the weak intermolecular interaction is small ($D_0 < 12$ kJ/mol).[11,13] The minor influence of microsolvation on the AH^+ properties may be controlled by either the systematic variation of L (e.g., the intermolecular interaction) or the comparison with calculations.[11−16]

In the present study, the protonation sites of isolated fluorobenzene (C_6H_5F) are investigated by IR spectroscopy and quantum chemical calculations. Figure 1 summarizes possible $C_6H_6F^+$ structures. Protonation may occur either at the aromatic ring in the ortho (o-$C_6H_6F^+$), meta (m-$C_6H_6F^+$), para (p-$C_6H_6F^+$), and ipso (i-$C_6H_6F^+$) positions to form carbenium ions (fluorobenzenium, Figure 1a−d) or at the F atom to form a fluoronium ion (F-$C_6H_6F^+$, phenylfluoronium, Figure 1i). These σ-complexes are minima on the potential energy surface (PES) calculated for $C_6H_6F^+$, and the lowest energy interconversion between them proceeds via hydrogen bridged transition

states (Figure 1e−h).[17,18] Similar to $C_6H_7^+$, π-complexes corresponding to face protonation above and below the aromatic ring are expected to be less stable saddle points and are not considered further.[11,19] Other less stable isomers on the PES of $C_6H_6F^+$ are HF−$C_6H_5^+$ ion−dipole complexes (Figure 1j−l), where $C_6H_5^+$ is the phenyl cation in its $^1A_1$ electronic ground state. The fluoronium ion (F-$C_6H_6F^+$, Figure 1i) can also be considered as such a weakly bound HF−$C_6H_5^+$ complex, because of its small dissociation energy with respect to the HF + $C_6H_5^+$ fragment channel (Figure 2). This low-energy channel opens the possibility to record the IR spectrum of isolated F-$C_6H_6F^+$ via IRPD spectroscopy, that is without any "messenger". The $C_6H_6F^+$ spectrum observed in the present work corresponds to the first IR spectroscopic detection of a protonated aromatic molecule completely free from interference with any solvation effect. The low dissociation energy of F-$C_6H_6F^+$ with respect to dehydrofluorination is an interesting example of C−F bond destabilization upon protonation. The inert C−F bond in stable fluorocarbons is apparently the strongest (single) bond that carbon can form.[20] Interestingly, this bond can be significantly weakened by attaching either a proton or a metal cation to the F atom, respectively.[21]

Low-temperature NMR spectra in superacid solutions revealed a static σ-complex of p-$C_6H_6F^+$, whereas complete scrambling of all ring protons was observed at higher temperature due to rapid intramolecular 1,2 H-shift.[18] Only carbenium ions of $C_6H_6F^+$ (o,m,p-$C_6H_6F^+$) were observed in the condensed phase, and no evidence for a π-complex or the fluoronium isomer was reported. All gas-phase experiments of $C_6H_6F^+$ are based solely on mass spectrometry[17,22−29] and demonstrate that the protonation sites observed strongly depend on the experimental conditions, such as pressure, temperature, and the Brønsted acid used for protonation. The proton affinities (PAs) for ring protonation (assumed to occur in para position) and F protonation were determined as 755.9 and 577 ± 24 kJ/mol, respectively.[25,30] Although F-$C_6H_6F^+$ is considerably less stable than all carbenium isomers (Figure 2), significant abundance of the former ion can be produced by chemical ionization of C_6H_5F using a protonating agent with a slightly smaller PA, such as CH_5^+ ($PA_{CH_4} = 543.5$ kJ/mol).[30] In addion to thermodynamic considerations, kinetic factors strongly affect the branching ratio between carbenium and fluoronium production using CH_5^+.[22,25,27,28] Once stable F-$C_6H_6F^+$ is formed, isomerization toward the more stable carbenium ions is strongly hindered by a high barrier (Figure 2). On the other hand, no

(13) Solcà, N.; Dopfer, O. *Chem. Phys. Lett.* **2001**, *342*, 191.
(14) Yeh, L. I.; Okumura, M.; Myers, J. D.; Price, J. M.; Lee, Y. T. *J. Chem. Phys.* **1989**, *91*, 7319.
(15) Nizkorodov, S. A.; Roth, D.; Olkhov, R. V.; Maier, J. P.; Dopfer, O. *Chem. Phys. Lett.* **1997**, *278*, 26.
(16) Olkhov, R. V.; Dopfer, O. *Chem. Phys. Lett.* **1999**, *314*, 215.

(17) Hrusak, J.; Schröder, D.; Weiske, T.; Schwarz, H. *J. Am. Chem. Soc.* **1993**, *115*, 2015.
(18) Olah, G. A.; Mo, Y. K. *J. Org. Chem.* **1973**, *38*, 3212.
(19) Szulejko, J. E.; Hrusak, J.; McMahon, T. B. *J. Mass Spectrom.* **1997**, *32*, 494.
(20) Hudlicky, M. *Chemistry of Organic Fluorine Compounds*; Prentice Hall: New York, 1992.
(21) Plenio, H. *Chem. Rev.* **1997**, *97*, 3363.
(22) Speranza, M.; Cacace, F. *J. Am. Chem. Soc.* **1977**, *99*, 3051.
(23) Cacace, F.; Speranza, M. *J. Am. Chem. Soc.* **1976**, *98*, 7299.
(24) Speranza, M.; Sefcik, M. D.; Henis, J. M. S.; Gaspar, P. P. *J. Am. Chem. Soc.* **1977**, *99*, 5583.
(25) Mason, R.; Milton, D.; Harris, F. *J. Chem. Soc., Chem. Commun.* **1987**, 1453.
(26) Tkaczyk, M.; Harrison, A. G. *Int. J. Mass Spectrom. Ion Processes* **1990**, *100*, 133.
(27) Tkaczyk, M.; Harrison, A. G. *Int. J. Mass Spectrom. Ion Processes* **1994**, *132*, 73.
(28) Mason, R. S.; Parry, A. J.; Milton, D. M. P. *J. Chem. Soc., Faraday Trans.* **1994**, *90*, 1373.
(29) Schröder, D.; Oref, I.; Hrusak, J.; Weiske, T.; Nikitin, E. E.; Zummack, W.; Schwarz, H. *J. Phys. Chem. A* **1999**, *103*, 4609.
(30) Hunter, E. P. L.; Lias, S. G. *J. Phys. Chem. Ref. Data* **1998**, *27*, 413.
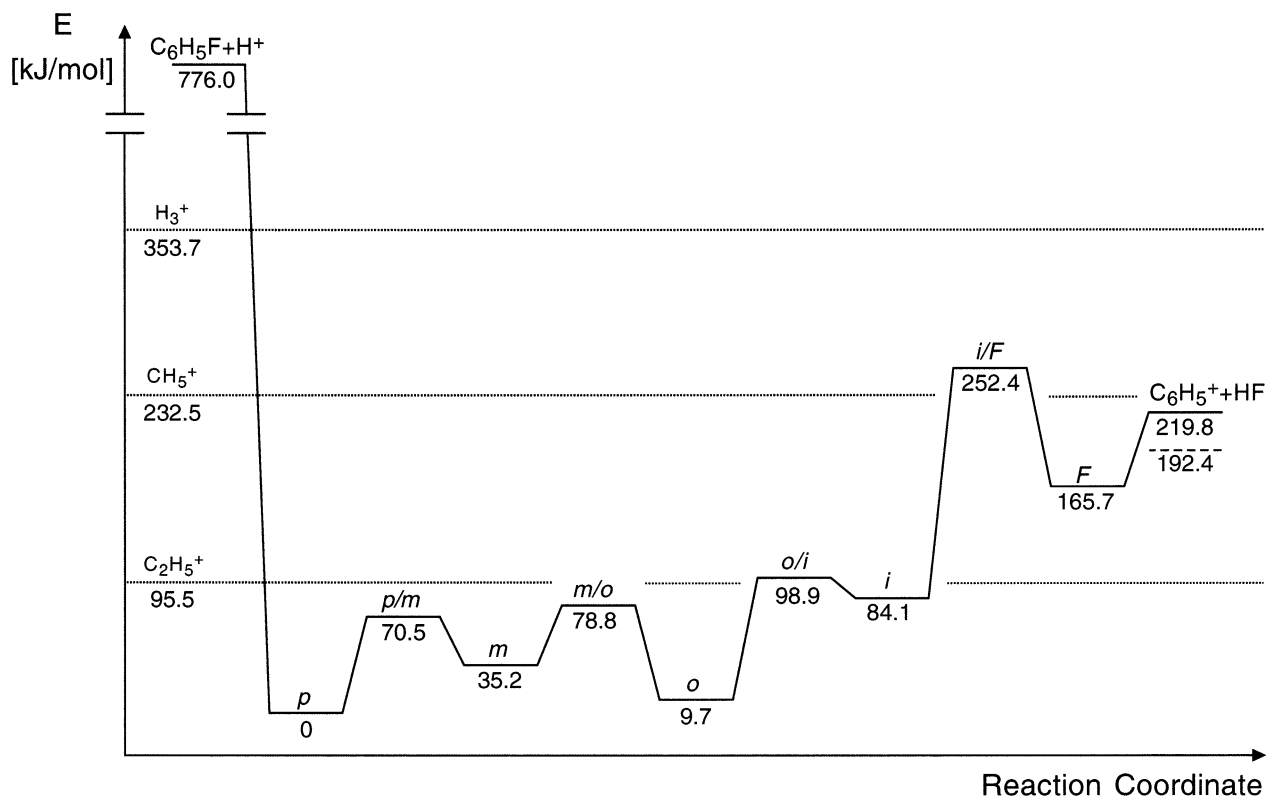
Figure 2. Salient parts of the PES of $C_6H_6F^+$ calculated at the B3LYP/6-311G(2df,2pd) level. Energies are corrected for zero point energy. See Figure 1 for the notation of the $C_6H_6F^+$ structures. The dashed line indicates the relative energy of $HF^{mo}-C_6H_5^+$. Experimental excess energies for protonation of C_6H_5F in the para position by H_3^+, CH_5^+, and $C_2H_5^+$ are indicated by dotted horizontal lines.[30] The lowest dissociation channel for all $C_6H_6F^+$ isomers corresponds to dehydrofluorination, that is, fragmentation into the electronic ground states of $C_6H_5^+$ ($^1A_1$) and HF ($^1\Sigma^+$).

evidence for F-$C_6H_6F^+$ generation was observed using stronger or weaker Brønsted acids, such as H_3^+ ($PA_{H_2} = 422.3$ kJ/mol) and $C_2H_5^+$ ($PA_{C_2H_4} = 680.5$ kJ/mol).[30] In the first case, this is probably due to the large excess energy involved in the proton-transfer reaction (Figure 2), leading to either dehydrofluorination or fast isomerization to carbenium ions.[28] In the second case, the energy of the Brønsted acid is simply too low to directly protonate the F atom, and solely carbenium ions are formed (Figure 2).[25,27,28]

In the present work, C_6H_5F is protonated by CH_5^+ to produce stable carbenium and fluoronium isomers of $C_6H_6F^+$. The energy required for dehydrofluorination (Figure 2) is on the order of the C−H and F−H stretch frequencies. Thus, resonant absorption of a single IR photon in the mid-IR range can populate predissociating vibrational levels of F-$C_6H_6F^+$, and this effect is exploited to record the IR spectrum of F-$C_6H_6F^+$ by IRPD spectroscopy. A similar approach was previously used to obtain gas-phase IR spectra of isolated polycyclic aromatic hydrocarbon cations (PAH$^+$).[31] In these studies, however, the fragmentation of PAH$^+$ is induced by sequential resonant absorption of more than 50−100 photons using intense IR pulses generated by a free electron laser.[31] The significantly lower laser intensities available in the present work are insufficient to drive multi-photon absorption processes. This situation is exploited for isomer selective photofragmentation of $C_6H_6F^+$ ions. The IRPD spectra of $C_6H_6F^+$ show only absorptions of the weakly bound F-$C_6H_6F^+$ isomer, whereas the more stable carbenium ions escape detection in the present experiment.

(31) Oomens, J.; Meijer, G.; von Helden, G. *J. Phys. Chem. A* **2001**, *105*, 8302.

2. Experimental and Theoretical Methods

IRPD spectra of mass-selected $C_6H_6F^+$ ions are recorded in a tandem mass spectrometer coupled to an electron ionization source and an octopole ion trap.[32] A pulsed supersonic expansion of C_6H_5F seeded in two different buffer gas mixtures at 8 bar stagnation pressure is crossed by two electron beams ($\sim$100 eV) close to the nozzle orifice. Mixture A contains CH_4/Ar in the ratio 1:1, and mixture B is composed of H_2/Ar in the ratio 1:25. Electron ionization and fast ion−molecule reactions produce Brønsted acids XH^+ in the high-pressure region of the expansion. The most probable production pathway for $C_6H_6F^+$ corresponds to exothermic proton transfer

$$XH^+ + C_6H_5F \rightarrow C_6H_6F^+ + X \tag{1}$$
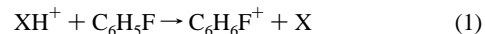
and subsequent stabilization by collisional cooling. The central part of the ion source plasma is extracted through a skimmer into a quadrupole mass spectrometer (QMS1) tuned to the mass of $C_6H_6F^+$ ($m = 97$ u). The mass-selected $C_6H_6F^+$ beam is injected into an octopole and exposed to an IR laser pulse with $\lambda \approx 3$ μm. Resonant excitation of $C_6H_6F^+$ into metastable vibrational levels leads to fragmentation into the phenyl cation ($C_6H_5^+$) and HF (dehydrofluorination), which is the lowest energy dissociation channel accessible for all $C_6H_6F^+$ isomers (Figure 2):[17]

$$C_6H_6F^+ + \nu_{IR} \rightarrow C_6H_5^+ + HF \tag{2}$$
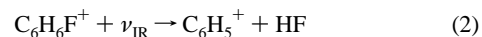
No other fragment channel is observed upon IR excitation. The $C_6H_5^+$ ions ($m = 77$ u) are filtered by a second quadrupole (QMS2) and monitored as a function of the laser frequency (ν_{IR}) to record the IR

(32) Nizkorodov, S. A.; Dopfer, O.; Ruchti, T.; Meuwly, M.; Maier, J. P.; Bieske, E. J. *J. Phys. Chem.* **1995**, *99*, 17118.

action spectrum of $C_6H_6F^+$. To suppress the background signal, mainly arising from metastable decay of initially hot parent ions in the octopole, the ion source is triggered at twice the laser frequency (20 Hz), and signals from alternating triggers are subtracted. IR radiation with 0.02 cm^{-1} bandwidth, 2500−6900 cm^{-1} tuning range, ~200 kW/cm² intensity, and ~5 ns pulse duration is generated by an optical parametric oscillator (OPO) laser system. Frequency calibration to better than 0.5 cm^{-1} is accomplished by optoacoustic spectra of HDO recorded with the signal output of the OPO and atmospheric water absorptions along the IR laser path.[33,34] The IR spectra are linearly normalized for laser intensity variations measured with an InSb detector.

Ab initio and density functional calculations[35] at the MP2(fc) and B3LYP levels using the 6-311G(2df,2pd) basis set are employed to explore the PES of $C_6H_6F^+$, with the main focus on the stability, structure, and spectroscopic properties of different isomers. All coordinates are relaxed during the search for stationary points. Relative energies and PAs (neglecting temperature effects) are corrected for zero point energies. For this purpose, harmonic frequencies are scaled by a factor of 0.96406 to match the calculated (4109.1 cm^{-1}, B3LYP) and experimental fundamental of HF (3961.42 cm^{-1}).[36] Intermolecular dissociation energies (D_e) of ion−dipole complexes are corrected for basis set superposition error,[37,38] and the substantial relaxation energy caused by the complexation induced deformation of the HF and $C_6H_5^+$ fragments.[39] As in nearly all cases the B3LYP and MP2 results are similar, only the B3LYP data are reported (if not stated otherwise).

3. Theoretical Results

The salient part of the $C_6H_6F^+$ PES is summarized in Figure 2. In agreement with previous calculations,[17,19,40−42] the relative energies of $C_6H_6F^+$ isomers vary in the order p-$C_6H_6F^+$ < o-$C_6H_6F^+$ ≪ m-$C_6H_6F^+$ ≪ i-$C_6H_6F^+$ ≪ F-$C_6H_6F^+$, reflecting the ortho/para directing nature of the F substituent upon electrophilic attack. Experimental PAs for ring and F protonation (755.9 and 577 ± 24 kJ/mol)[25,30] are slightly smaller than the calculated PAs for p-$C_6H_6F^+$ and F-$C_6H_6F^+$ (776.0 and 610.3 kJ/mol). Moreover, the B3LYP level appears to reproduce the barriers for proton migration well: for example, the calculated barrier for the 1,2 H-shift in $C_6H_7^+$ (38.4 kJ/mol)[43] is close to the experimental value in solution (42 ± 5 kJ/mol).[44] Consequently, the B3LYP level is concluded to correctly reproduce the topology of the $C_6H_6F^+$ PES.[45] The carbenium ions

are well separated from F-$C_6H_6F^+$ by a substantial barrier of ~100 kJ/mol, associated with a large imaginary frequency of the i/F-$C_6H_6F^+$ transition state along the proton migration coordinate (1566i cm^{-1}). Barriers between the carbenium isomers are lower (15−89 kJ/mol), with correspondingly smaller frequencies (810i ± 40i cm^{-1}). Figure 2 also includes the experimental excess energies for protonation of C_6H_5F in the para position by H_3^+, CH_5^+, and $C_2H_5^+$.[30] All three considered Brønsted acids may produce carbenium ions via reaction 1, whereas F protonation is energetically only feasible using H_3^+ and CH_5^+.[25,27,28]

The lowest fragmentation channel for $C_6H_6F^+$ corresponds to dehydrofluorination, that is, dissociation into HF and the phenyl cation ($C_6H_5^+$) in their singlet electronic ground states.[17,46] The small calculated dissociation energy for F-$C_6H_6F^+$ of D_0 = 54.1 kJ/mol (4521 cm^{-1}) implies that this cation can be considered as an electrostatic ion−dipole complex, HF−$C_6H_5^+$. For comparison, the related water−benzene cation complex (H_2O−$C_6H_6^+$) has a similar binding energy, $D_0 \approx 58$ ± 13 kJ/mol.[47] In contrast to fluoronium, fragmentation of the carbenium isomers into HF and $C_6H_5^+$ involves high barriers (>168 kJ/mol) and much larger dissociation energies (136−220 kJ/mol). Consequently, the carbenium ions are not detected in the present photofragmentation experiment, and their theoretical properties are not discussed in detail further.

Figure 3 compares the geometries of C_6H_5F (¹A₁, C_{2v}), F-$C_6H_6F^+$ (¹A′, C_s), and $C_6H_5^+$ (¹A₁, C_{2v}) in their electronic ground states to illustrate the structural effects of (de)protonation and (de)hydrofluorination, respectively. In agreement with previous HF/6-31G* calculations,[17] the F−H bond of F-$C_6H_6F^+$ lies in a plane perpendicular to the ring with a H−F−C angle of 113°. The weak C−F bond is substantially longer than that in C_6H_5F (1.691 vs 1.346 Å), justifying the description of F-$C_6H_6F^+$ as a HF−$C_6H_5^+$ ion−dipole complex. A similar destabilization of the C−F bond is also observed when metal ions (such as Li^+) are attached to the F atom of fluorinated aromatic molecules.[21] The atoms-in-molecules population analysis of the charge distribution in F-$C_6H_6F^+$ indicates that the charge of the added proton is nearly completely delocalized over the $C_6H_5^+$ ring, in line with the lower ionization potential of C_6H_5 as compared to that of HF (8.25 and 16.04 eV).[48] As only +0.17 e remains on the FH group, the F−H bond in F-$C_6H_6F^+$ is only slightly weaker and longer than that in bare HF (by 0.023 Å), but it is still substantially stronger and shorter than that in HF^+ (−0.069 Å). Most geometric data of the F-$C_6H_6F^+$ ring are bracketed by those of C_6H_5F and $C_6H_5^+$, which result from H^+ and HF loss of F-$C_6H_6F^+$ (Figure 3). In contrast to the geometries of the ring skeleton, the C−H bond lengths are rather similar in C_6H_5F, F-$C_6H_6F^+$, and $C_6H_5^+$. Apparently, F protonation of C_6H_5F drastically reduces the covalent character of the C−F bond, resulting in a compression of the six-membered ring. The substantial structural change of $C_6H_5^+$ upon HF complexation amounts to a large relaxation energy of 2550 cm^{-1}. The geometries evaluated at the MP2 and B3LYP levels are very similar, with the exception that the MP2 level predicts a shorter C−F bond in F-$C_6H_6F^+$ (1.609 vs 1.691 Å). Interest-

(33) Guelachvili, G.; Rao, K. N. *Handbook of Infrared Standards*; Academic Press: London, 1993.
(34) Camy-Peyret, C.; Flaud, J. M.; Guelachvili, G.; Amiot, C. *Mol. Phys.* **1973**, *26*, 825.
(35) Frisch, M. J.; Trucks, G. W.; Schlegel, H. B.; Scuseria, G. E.; Robb, M. A.; Cheeseman, J. R.; Zakrzewski, V. G.; Montgomery, J. A., Jr.; Stratmann, R. E.; Burant, J. C.; Dapprich, S.; Millam, J. M.; Daniels, A. D.; Kudin, K. N.; Strain, M. C.; Farkas, O.; Tomasi, J.; Barone, V.; Cossi, M.; Cammi, R.; Mennucci, B.; Pomelli, C.; Adamo, C.; Clifford, S.; Ochterski, J.; Petersson, G. A.; Ayala, P. Y.; Cui, Q.; Morokuma, K.; Malick, D. K.; Rabuck, A. D.; Raghavachari, K.; Foresman, J. B.; Cioslowski, J.; Ortiz, J. V.; Stefanov, B. B.; Liu, G.; Liashenko, A.; Piskorz, P.; Komaromi, I.; Gomperts, R.; Martin, R. L.; Fox, D. J.; Keith, T.; Al-Laham, M. A.; Peng, C. Y.; Nanayakkara, A.; Gonzalez, C.; Challacombe, M.; Gill, P. M. W.; Johnson, B. G.; Chen, W.; Wong, M. W.; Andres, J. L.; Head-Gordon, M.; Replogle, E. S.; Pople, J. A. *Gaussian 98*, revision A.7; Gaussian, Inc.: Pittsburgh, PA, 1998.
(36) Le Blanc, R. B.; White, J. B.; Bernath, P. F. *J. Mol. Spectrosc.* **1994**, *164*, 574.
(37) Boys, S. F.; Bernardi, F. *Mol. Phys.* **1970**, *19*, 553.
(38) Although the energies are corrected for BSSE, the equilibrium geometries are not.
(39) Chalasinski, G.; Szczesniak, M. M. *Chem. Rev.* **1994**, *94*, 1.
(40) Bader, R. F. W.; Chang, C. *J. Phys. Chem.* **1989**, *93*, 5095.
(41) Maksic, T. B.; Kovacevic, B.; Kovacek, D. *J. Phys. Chem. A* **1997**, *101*, 7446.
(42) Wiberg, K. B.; Rablen, P. R. *J. Org. Chem.* **1998**, *63*, 3722.
(43) Dopfer, O., unpublished results.
(44) Olah, G. A.; Staral, J. S.; Asencio, G.; Liang, G.; Forsyth, D. A.; Mateescu, G. D. *J. Am. Chem. Soc.* **1978**, *100*, 6299.
(45) Tishchenko, O.; Pham-Tran, N. N.; Kryachko, E. S.; Nguyen, M. T. *J. Phys. Chem. A* **2001**, *105*, 8709.

(46) Winkler, M.; Sander, W. *Angew. Chem., Int. Ed.* **2000**, *39*, 2014.
(47) Solcà, N.; Dopfer, O. *Chem. Phys. Lett.* **2001**, *347*, 59.
(48) Lias, S. G.; Bartmess, J. E.; Liebman, J. F.; Holmes, J. L.; Levin, R. D.; Mallard, W. G. *J. Phys. Chem. Ref. Data* **1984**, *13*, 695.
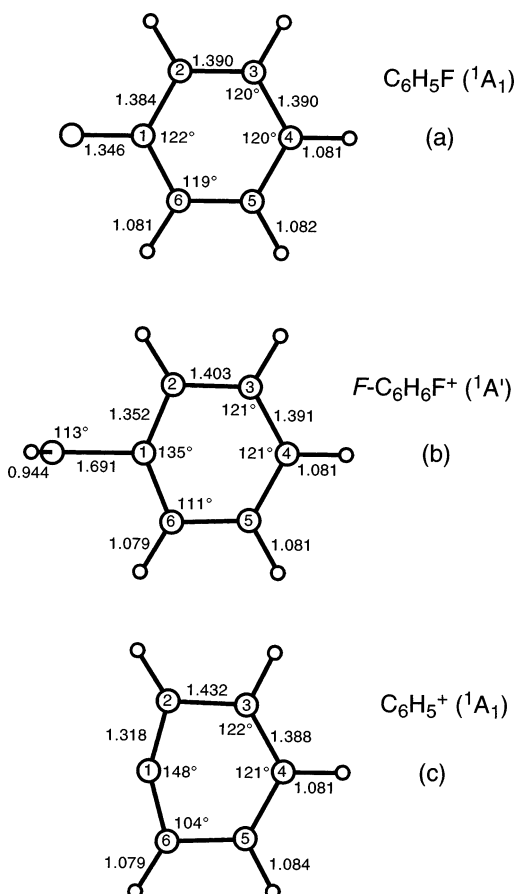
Figure 3. Structures (in Å and deg) of (a) C_6H_5F ($^1A_1$, C_{2v}), (b) F-$C_6H_6F^+$ ($^1A'$, C_s), and (c) $C_6H_5^+$ ($^1A_1$, C_{2v}) in their electronic ground states calculated at the B3LYP/6-311G(2df,2pd) level.

Table 1. Scaled Harmonic Vibrational Frequencies (Scaling Factor 0.96406), IR Intensities (km/mol, in Parentheses), and Symmetry Species of Fundamental Vibrations of F-$C_6H_6F^+$ in Its Electronic Ground State ($^1A'$, C_s) Calculated at the B3LYP/6-311G(2df,2pd) Level

ν [cm^{-1}]	symmetry	ν [cm^{-1}]	symmetry	ν [cm^{-1}]	symmetry
185 (7)	A′	783 (179)	A′	1285 (7)	A″
188 (148)	A″	876 (2)	A′	1403 (70)	A′
270 (1)	A″	887 (63)	A′	1442 (10)	A″
288 (70)	A′	950 (0)	A″	1489 (1)	A′
409 (1)	A″	979 (4)	A′	1638 (21)	A″
425 (18)	A′	991 (0)	A′	3081 (2)	A′
550 (2)	A″	1022 (0)	A′	3086 (1)	A″
592 (51)	A′	1032 (3)	A″	3096 (7)	A′
620 (2)	A′	1127 (2)	A′	3111 (53)	A″
707 (100)	A′	1146 (0)	A″	3112 (5)	A′
710 (1)	A″	1234 (20)	A″	3642 (492)	A′

ingly, the corresponding dissociation energies nearly match (D_e = 5583 vs 5793 cm^{-1}).

Table 1 lists the vibrational frequencies and IR intensities of F-$C_6H_6F^+$. The F–H stretch (σ_{FH}) is predicted to be the most intense IR-active fundamental. Its frequency (3642 cm^{-1}) lies much closer to that of free HF (3961 cm^{-1}) than to that of bare HF$^+$ (2885 cm^{-1}), consistent with the small charge transfer in the HF–$C_6H_5^+$ notation of F-$C_6H_6F^+$. In addition to σ_{FH}, the antisymmetric C–H stretch of the C2–H and C6–H bonds, σ_{CH} = 3111 cm^{-1}, is the only other fundamental with significant IR intensity in the investigated 3 μm range. This mode has almost the same frequency as that in $C_6H_5^+$ (σ_{CH} = 3110 cm^{-1}), in line with the similar C–H bond lengths (Figure 3). In contrast,

all other normal modes of F-$C_6H_6F^+$ display significantly larger frequency shifts, because of the substantial $C_6H_5^+$ deformation upon HF complexation. The weak C–F bond in F-$C_6H_6F^+$ results in low frequencies of the corresponding (intermolecular) normal modes. The C–F stretch frequency (σ_{CF} = 288 cm^{-1}) is much smaller than those in other monosubstituted benzene derivatives (C_6H_5X), for which generally $\sigma_{CX} > 1000$ cm^{-1} for substituents with $m(X) < 25$ u.[49] The two C–F bending frequencies are β_{CF}(a′) = 185 cm^{-1} and β_{CF}(a″) = 270 cm^{-1}, and the F–H torsions corresponding to hindered internal FH rotation are τ_{FH}(a′) = 783 cm^{-1} and τ_{FH}(a″) = 188 cm^{-1}.

In addition to F-$C_6H_6F^+$ (D_0 = 4521 cm^{-1}), three less stable ion–dipole complexes with C_s symmetry are identified as local minima on the intermolecular HF–$C_6H_5^+$ PES (Figure 1j–l). In the latter dimers, the electrostatic charge–dipole force dominates the attraction, and the HF dipole points toward the $C_6H_5^+$ cation. In HF$^\pi$–$C_6H_5^+$, the HF ligand forms a π-bond to the $C_6H_5^+$ ring with a separation of 2.88 Å and a binding energy of D_0 = 1595 cm^{-1}. The planar HF^{pm}–$C_6H_5^+$ and HF^{mo}–$C_6H_5^+$ dimers feature slightly asymmetric bifurcated H-bonds with D_0 = 1851 and 2293 cm^{-1}, respectively. As an example, the energy of HF^{mo}–$C_6H_5^+$ is included in Figure 2 (dashed line). Clearly, these three HF–$C_6H_5^+$ isomers may also be detected in the present experimental scheme, as $D_0 < \nu_{IR} \approx 3 \times 10^3$ cm^{-1}. In this frequency range, the vibrational properties of HF$^\pi$–$C_6H_5^+$, HF^{pm}–$C_6H_5^+$, and HF^{mo}–$C_6H_5^+$ are very similar. As a consequence of the weak intermolecular interaction, their F–H stretch frequencies (σ_{FH} = 3895–3905 cm^{-1}) are predicted to be relatively close to that of free HF (σ_{FH} = 3961 cm^{-1}), and the intense antisymmetric σ_{CH} fundamentals (σ_{CH} = 3115 ± 1 cm^{-1}) lie very close to that of bare $C_6H_5^+$ (σ_{CH} = 3110 cm^{-1}). The only exception is HF^{mo}–$C_6H_5^+$ (σ_{CH} = 3099 cm^{-1}), because one ortho H atom is involved in the bifurcated H-bond. In general, the frequency shifts and IR intensities of σ_{FH} of the three HF–$C_6H_5^+$ isomers are lower than those in F-$C_6H_6F^+$ because of the weaker interaction in the former complexes.

The long-range attraction of the HF–$C_6H_5^+$ PES is dominated by electrostatic and induction forces between the positive charge (q) distributed in $C_6H_5^+$ and the permanent multipole moments and polarizability of HF (dipole $\mu \approx 1.8$ D, quadrupole $\Theta \approx 2.4$ DÅ, $\alpha \approx 0.8$ Å^3).[50] The anisotropy of the q–μ and q–α attraction favors a linear over a T-shaped orientation.[12] The weakly bound HF$^\pi$–$C_6H_5^+$, HF^{pm}–$C_6H_5^+$, and HF^{mo}–$C_6H_5^+$ isomers indeed have equilibrium structures in which the HF dipole points away from $C_6H_5^+$. However, in the more strongly bound F-$C_6H_6F^+$, the H–F–C angle (113°) deviates substantially from 180°, indicating that other interactions must be significant. Indeed, at shorter range, the q–Θ interaction as well as covalent contributions may be important. The anisotropy of the q–Θ force favors a T-shaped over the linear configuration and may cause the deviation from linearity.[12] In addition, a bent H–F–C structure is expected in the limit of chemical bonding, arising from dative bonding between a lone pair of F and the very electrophilic $C_6H_5^+$ ion.[51] For example, the bond angle in the related HFH$^+$ cation (113 ± 2°)[52] is very similar to that calculated for F-$C_6H_6F^+$. In contrast to symmetric HFH$^+$,

(49) Varsanyi, G. *Assignments for Vibrational Spectra of 700 Benzene Derivatives*; Adam Hilger: London, 1974.
(50) Gray, C. G.; Gubbins, K. E. *Theory of Molecular Fluids*; Clarendon: Oxford, 1984; Vol. 1.

F-C₆H₆F⁺ does not feature a fully developed chemical bond as is demonstrated by the weak and long C−F bond. The large difference in the dissociation energies of HF−H⁺ ($D_0 \approx PA_{HF}$ = 484 kJ/mol)[30] and HF−C₆H₅⁺ ($D_0 \approx 54$ kJ/mol) reflects the drastic effect upon substitution of H⁺ by C₆H₅⁺. Nonetheless, incipient chemical bonding is indicated by the substantial deformation of C₆H₅⁺ upon HF complexation and the partial charge transfer from C₆H₅⁺ to HF. In general, the strength of the (intermolecular) C−L bond in L−C₆H₅⁺ strongly depends on the ligand L.[53] Interestingly, although N₂ is usually more inert than HF, with smaller permanent multipole moments (μ = 0, $\Theta \approx -1.5$ DÅ),[50] the interaction in the N₂−C₆H₅⁺ diazonium ion, an exceptionally stable and widespread reagent in organic synthesis,[1] is calculated to be roughly twice stronger than that in *F*-C₆H₆F⁺ (D_0 = 10 070 vs 4521 cm⁻¹), because of stronger dative bonding.[53] In contrast to N₂−C₆H₅⁺, to the best of our knowledge, *F*-C₆H₆F⁺ has never been observed in the condensed phase.

4. Experimental Results and Discussion

4.1. Mass Spectra. Mass spectra of the ion source obtained by seeding C₆H₅F with mixtures A and B are displayed in Figure 4a and b, respectively. Using mixture B, we found that the major protonating agents are H₃⁺ and ArH⁺, and the mass spectrum in Figure 4b is dominated by Ar⁺ and ArH⁺, C₆H₅F⁺ and its fragment ions (●),[54] and C₆H₆F⁺ with its intense C₆H₅⁺ fragment. In addition, the peak at 79 u (○) is assigned to C₆H₇⁺, originating from the reaction between H₃⁺ and C₆H₅F with subsequent HF loss.[55] Different protonating agents are produced using CH₄ in the expansion (mixture A), the most abundant being CH₅⁺ and C₂H₅⁺.[56−60] Consequently, both ions occur in the mass spectrum with high intensity, along with C₆H₅F⁺, C₆H₆F⁺, and their fragment ions (Figure 4a). The reaction between CH₅⁺ and C₆H₅F with subsequent HF loss leads to C₇H₉⁺ (93 u, ○).[55] Apparently, less fragmentation of C₆H₅F⁺ is observed using CH₄ instead of Ar/H₂ because of softer chemical ionization.[55] Significantly, fragmentation of C₆H₆F⁺ protonated by H₃⁺/ArH⁺ leads also to a much higher C₆H₅⁺ fragment peak than does protonation by CH₅⁺/C₂H₅⁺. The latter observation is consistent with the higher PAs of CH₄/C₂H₄ (as compared to those of H₂/Ar), which leave C₆H₆F⁺ with less internal energy after protonation (Figure 2).

Figure 5 shows mass spectra obtained by selecting C₆H₆F⁺ with QMS1 and scanning QMS2 to monitor metastable decay (MD), resonant laser-induced dissociation (LID), and collision-induced dissociation (CID). MD originates from fragmentation of initially hot C₆H₆F⁺ ions in the octopole which survive the passage through QMS1 as parent ions (∼500 µs). CID spectra are obtained by introducing He collision gas into the octopole
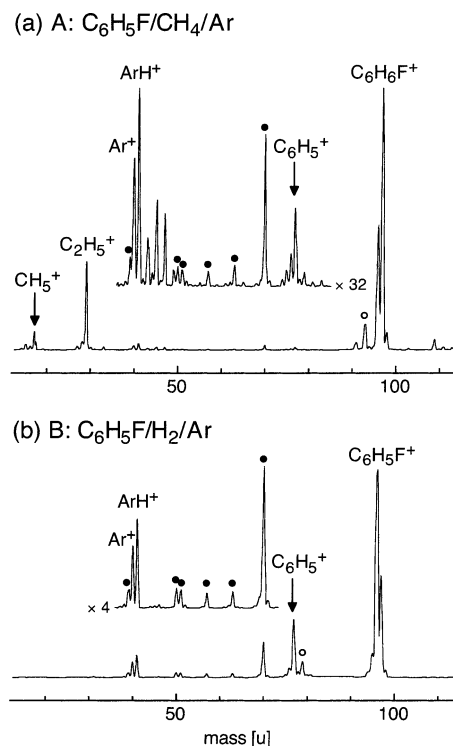

(a) A: C₆H₅F/CH₄/Ar

(b) B: C₆H₅F/H₂/Ar

Figure 4. Mass spectra of the electron ionization source for an expansion of C₆H₅F seeded with (a) mixture A (CH₄/Ar ratio is 1:1) and (b) mixture B (H₂/Ar ratio is 1:25) at 8 bar stagnation pressure. Fragment ions of C₆H₅F⁺ are indicated by ●. The most intense peaks in spectrum (a) are assigned to C₆H₆F⁺, C₆H₅F⁺, CH₅⁺, C₂H₅⁺, and C₇H₉⁺ (○). All major peaks in spectrum (b) are assigned to C₆H₅F⁺ and its fragment ions,[54] C₆H₆F⁺, C₆H₅⁺, Ar⁺/ArH⁺, and C₆H₇⁺ (○).[55] Part of the spectra (a) and (b) are vertically expanded by factors of 32 and 4, respectively, to visualize small peaks.
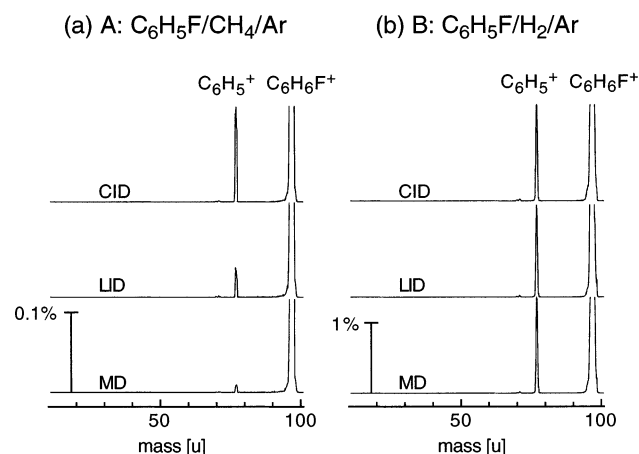

(a) A: C₆H₅F/CH₄/Ar   (b) B: C₆H₅F/H₂/Ar

Figure 5. Mass spectra obtained by mass selecting C₆H₆F⁺ (97 u) with QMS1 and scanning QMS2 using (a) mixture A (CH₄/Ar ratio is 1:1) and (b) mixture B (H₂/Ar ratio is 1:25) to monitor metastable decay (MD), laser-induced dissociation (LID, laser tuned to ν_{IR} = 3645 cm⁻¹), and collision-induced dissociation (CID, collision energy is ∼0.29 eV in the center-of-mass frame) of C₆H₆F⁺. The weak signals in the mass channels 70 and 71 u are attributed to ¹³C¹²CH₂ and ¹²C₂H₂ loss of ¹³C¹²C₅H₅F⁺, which slightly contaminates the isobaric C₆H₆F⁺ (¹²C₆H₅FH⁺) mass channel. The signal intensities (in %) are normalized with respect to the corresponding parent ion yields. The scaling factors for vertical expansion in both series of spectra differ by roughly 1 order of magnitude.

(∼2 × 10⁻⁵ mbar, 0.29 ± 0.02 eV average center-of-mass collision energy). For LID spectra, the laser is set resonant to the F−H stretch of *F*-C₆H₆F⁺ at 3645 cm⁻¹. The mass spectra in Figure 5a and b are recorded using mixtures A and B,

(51) One can actually consider also dative bonding between C₆H₅F and H⁺ to rationalize a bent H−F−C configuration in *F*-C₆H₆F⁺. However, as the C−F bond in *F*-C₆H₆F⁺ is weak and the F−H bond is strong and similar to that in bare HF, *F*-C₆H₆F⁺ is better described by HF−C₆H₅⁺ than by C₆H₅F−H⁺.
(52) Schäfer, E.; Saykally, R. J. *J. Chem. Phys.* **1984**, *81*, 4189.
(53) Glaser, R.; Horan, C. J. *J. Org. Chem.* **1995**, *60*, 7518.
(54) NIST Chemistry Web Book; http://webbook.nist.gov, 2001.
(55) Harrison, A. G.; Lin, P. H. *Can. J. Chem.* **1975**, *53*, 1314.
(56) Abramson, F. P.; Furtell, J. H. *J. Chem. Phys.* **1966**, *45*, 1925.
(57) Chong, S. L.; Franklin, J. L. *J. Chem. Phys.* **1971**, *55*, 641.
(58) Huntress, W. T. *J. Chem. Phys.* **1972**, *56*, 5111.
(59) Weiner, J.; Smith, G. P. K.; Saunders, M.; Cross, R. J. *J. Am. Chem. Soc.* **1973**, *95*, 4115.
(60) Lee, H. S.; Bierbaum, V. M.; DePuy, C. H. *Int. J. Mass Spectrom. Ion Processes* **1997**, *167/168*, 587.
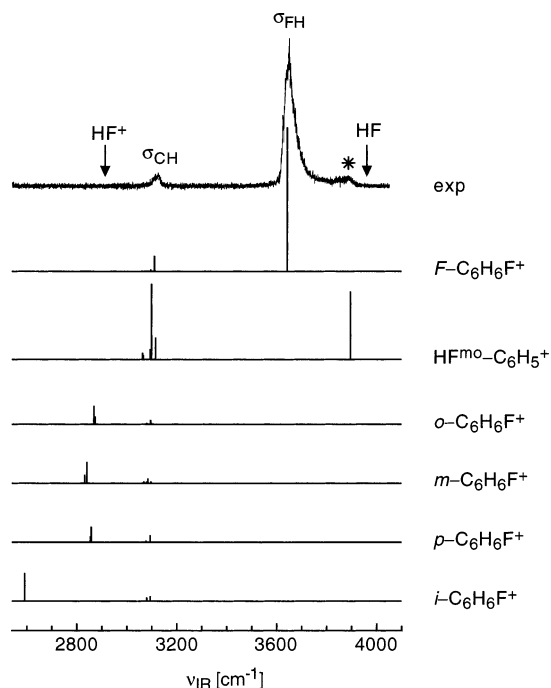
Figure 6. Experimental IRPD spectrum of $C_6H_6F^+$ between 2540 and 4050 cm^{-1} recorded in the $C_6H_5^+$ fragment channel as compared to stick spectra of the fluoronium isomer (F-$C_6H_6F^+$), the HF^{mo}-$C_6H_5^+$ ion-dipole complex, and the o,m,p,i-$C_6H_6F^+$ carbenium isomers (see Figure 1) calculated at the B3LYP/6-311G(2df,2pd) level. The relative intensities in the stick spectra of different isomers reflect directly the calculated IR oscillator strengths. The F-H stretch fundamentals of HF and HF$^+$ at 3961.4 and 2912.5 cm^{-1} are indicated by arrows.[36,61] The assignment of the band marked with an asterisk is ambiguous (Table 2).

respectively. In agreement with previous low-energy CID studies,[26,27] the dominant fragment ion in both MD and low-energy CID spectra in Figure 5 is $C_6H_5^+$ (HF loss). The $C_6H_5^+$ MD signal is much more intense using mixture B than mixture A, as protonation with H_3^+/ArH^+ deposits more excess energy in $C_6H_6F^+$ than does protonation with $CH_5^+/C_2H_5^+$ (Figure 2).[28] In fact, the MD signals using mixture B produce such a high background that additional CID and LID signals could not be distinguished within the signal-to-noise ratio obtained (Figure 5b). In contrast, using mixture A, we found that both LID and CID signals are much stronger than the MD background due to production of colder $C_6H_6F^+$ ions (Figure 5a). Consequently, this mixture is used for recording the IR spectra of $C_6H_6F^+$. The corresponding LID spectrum in Figure 5a shows that it is indeed possible to observe photodissociation of at least one $C_6H_6F^+$ isomer in the 3 μm range in the $C_6H_5^+$ fragment channel. The LID and CID spectra confirm that only this fragment channel is accessible by both resonant IR excitation and low-energy collisions under the present experimental conditions.[26] Consequently, the IR spectra of $C_6H_6F^+$ are monitored in this fragment channel (eq 2). Analysis of the mass spectra in Figures 4a and 5a (mixture A) reveals that the contamination of the $^{12}C_6H_6F^+$ mass channel (97 u) by $^{13}C^{12}C_5H_5F^+$ is less than 3%. This small contamination is, however, not relevant for the present study, because the very endothermic dehydrofluorination of $C_6H_5F^+$ cannot be observed in the present work.[54]

4.2. IR Spectra. The IRPD spectrum of $C_6H_6F^+$ between 2540 and 4050 cm^{-1} is shown in Figure 6. The band maxima, widths, and suggested assignments of the transitions observed

Table 2. Band Maxima, Widths (fwhm), and Assignments of the Vibrational Transitions Observed in the IR Photodissociation Spectrum of $C_6H_6F^{+\ a}$

ν [cm^{-1}]	width	assignment
3645	45	σ_{FH} of F-$C_6H_6F^+$
3125	30	σ_{CH} of F-$C_6H_6F^+$
3885^b	52	σ_{FH} of HF-$C_6H_5^+$
		$\sigma_{FH} + \sigma_x$ of F-$C_6H_6F^+$
		$\sigma_{CH} + \sigma_y$ of F-$C_6H_6F^+$

^{a} For asymmetric peaks, the band maximum differs from the band center.
^{b} The assignment of this band is tentative (see text for details).

are listed in Table 2. The assignments are based on the comparison with stick spectra calculated for different $C_6H_6F^+$ isomers. Figure 6 includes simulations for F-$C_6H_6F^+$, all carbenium isomers of $C_6H_6F^+$, and HF^{mo}-$C_6H_5^+$. As the spectra of the other two ion-dipole complexes HF^{pm}-$C_6H_5^+$ and HF$^\pi$-$C_6H_5^+$ are very similar to that of HF^{mo}-$C_6H_5^+$, they are not plotted in Figure 6.

On the basis of its position and IR intensity, the strong band observed at 3645 cm^{-1} is unambiguously assigned to the F-H stretch (σ_{FH}) of F-$C_6H_6F^+$. The calculations predict only for this isomer an intense fundamental in this frequency range. The frequency shift relative to free HF ($\Delta\sigma_{FH} = -316$ cm^{-1}) is in excellent agreement with the calculated value ($\Delta\sigma_{FH} = -319$ cm^{-1}). As predicted by the calculations, σ_{FH} of F-$C_6H_6F^+$ is much closer to σ_{FH} of HF (3961.4 cm^{-1})[36] than to σ_{FH} of HF$^+$ (2912.5 cm^{-1}),[61] confirming the modest charge transfer from $C_6H_5^+$ to HF. Similarly, σ_{FH} of F-$C_6H_6F^+$ is much higher than the average F-H stretch frequency in HFH$^+$, $\nu_{av} = 3341.7$. cm^{-1},[52] demonstrating the stabilizing effect of charge delocalization on the F-H bond upon substituting H$^+$ by $C_6H_5^+$. Indeed, PA$_{C_6H_5F}$ for F protonation (577 $\pm$ 24 kJ/mol) is larger than PA$_{HF}$ (484 kJ/mol).[25,30] The second transition observed at 3125 cm^{-1} is assigned to the antisymmetric C-H stretch of the two ortho H atoms of F-$C_6H_6F^+$ (σ_{CH}) and compares favorably with the calculated value of 3111 cm^{-1}. In addition to frequencies and relative IR intensities, both assignments are supported by the observed band profiles. The σ_{FH} transition is relatively broad (45 cm^{-1}), implying that the detected F-$C_6H_6F^+$ ions contain a certain amount of (ro)vibrational internal energy prior to photoexcitation. Moreover, this band is shaded to the blue, indicating that the rotational constants in the $\upsilon_{FH} = 1$ state are larger than those in the ground vibrational state. Because of anharmonicity, the vibrationally averaged F-H distance in the $\upsilon_{FH} = 1$ state is larger than that in the $\upsilon_{FH} = 0$ state. For free HF and HF$^+$, the corresponding elongation is $\Delta R_{FH} \approx 0.02$ Å.[36,61] To estimate the magnitude of this effect on the rotational constants of F-$C_6H_6F^+$, optimized geometries are calculated for various F-H separations by relaxing all other coordinates. The major structural change upon increasing R_{FH} by 0.02 Å is a significant contraction of the C-F bond ($\Delta R_{CF} = -0.008$ Å). The derived changes in the rotational constants upon σ_{FH} excitation are $\Delta A \approx 0.8 \times 10^{-5}$ cm^{-1} ($<$0.01%), $\Delta B \approx 15.6 \times 10^{-5}$ cm^{-1} (0.20%), and $\Delta C \approx 8.9 \times 10^{-5}$ cm^{-1} (0.16%). Band contour simulations of the σ_{FH} fundamental hybrid transition for $T = 100-500$ K result indeed in a slightly blue-shaded band profile. However, the total width of the transition cannot solely be attributed to unresolved rotational substructure. Another contribution arises from sequence transitions of the form σ_{FH}

(61) Hovde, D. C.; Keim, E. R.; Saykally, R. J. *Mol. Phys.* **1989**, *68*, 599.

$+ v_x \leftarrow v_x$, which occur at slightly higher frequencies than does the σ_{FH} fundamental. This is particularly true for vibrations v_x involving the C−F bond,[12] which correspond to intermolecular modes in the HF−$C_6H_5^+$ notation of F-$C_6H_6F^+$. Excitation of σ_{FH} causes the intermolecular C−F bond to become stronger and stiffer. For example, the C−F bond contraction upon σ_{FH} excitation ($\Delta R_{CF} \approx -0.01$ Å) implies that the C−F stretch frequency (σ_{CF}) in the $v_{FH} = 1$ state is larger than that in the $v_{FH} = 0$ state by ~ 10 cm^{-1}. Similar conclusions apply to the intermolecular bending and torsional vibrations, β_{CF} and τ_{FH}, as well as most low-frequency intramolecular modes. Moreover, the stronger C−F bond in the $v_{FH} = 1$ state is consistent with the magnitude of $\Delta \sigma_{FH}$. In the limit of adiabatic separation between inter- and intramolecular modes, $\Delta \sigma_{FH}$ corresponds to the increase of the intermolecular binding energy upon σ_{FH} excitation. Thus, assuming a ground-state dissociation energy of $D_0 = 4521$ cm^{-1} (B3LYP), the red shift of $\Delta \sigma_{FH} = -316$ cm^{-1} implies that the dissociation energy increases by $\sim 7\%$ in the $v_{FH} = 1$ state ($D_0 = 4837$ cm^{-1}). In contrast to σ_{FH}, the σ_{CH} band features a narrower (30 cm^{-1}) and more symmetric profile, suggesting that vibrational couplings between σ_{CH} and σ_x are smaller than those for σ_{FH}. This is consistent with a much smaller frequency shift upon HF complexation. Indeed, σ_{CH} of HF−$C_6H_5^+$ (3125 cm^{-1}) is very close to σ_{CH} of $C_6H_5^+$ isolated in an Ar matrix (3110 cm^{-1}),[46] confirming the weak coupling between σ_{CH} and the intermolecular modes. Finally, it is noted that a minor part of the signal around 3120 cm^{-1} may also arise from other, less IR intense C−H stretch modes of F-$C_6H_6F^+$ (Table 1, Figure 6).

In contrast to σ_{FH} and σ_{CH} of F-$C_6H_6F^+$, the interpretation of the weak and broad band (52 cm^{-1}) observed around 3880 cm^{-1} (marked by an asterisk in Figure 6) is ambiguous. Possible assignments include combination bands of F-$C_6H_6F^+$ (not included in the simulations) or the F−H stretch fundamentals of less stable HF−$C_6H_5^+$ complexes. As discussed below, an assignment to carbenium isomers can safely be excluded. According to Table 1, first overtones of F-$C_6H_6F^+$ are not expected in the 3500−5000 cm^{-1} range. Possible combination bands of F-$C_6H_6F^+$ near 3885 cm^{-1} include $\sigma_{FH} + v_x$, where v_x are intermolecular modes with a frequency of ~ 240 cm^{-1}. Indeed, the calculations predict several vibrations with similar frequencies and large IR intensities, such as the C−F stretch ($\sigma_{CF} = 288$ cm^{-1}) and the asymmetric FH torsion ($\tau_{FH}(a'') = 188$ cm^{-1}). In line with the large red shift $\Delta \sigma_{FH}$ and the calculations of F-$C_6H_6F^+$ structures with varying F−H bond lengths, both vibrations may strongly couple with σ_{FH}, giving rise to significant IR intensity for the corresponding combination bands. Alternatively, the 3885 cm^{-1} transition may be attributed to a $\sigma_{CH} + v_y$ combination band, where $v_y \approx 760$ cm^{-1}. Such bands may acquire additional IR intensity by Coriolis or Fermi interaction with the intense σ_{FH} vibration.[62,63] Possible candidates for v_y include the strongly IR-active symmetric FH torsion, $\tau_{FH}(a') = 783$ cm^{-1} (Table 1).

In a second scenario, the 3885 cm^{-1} band may be assigned to the F−H stretch fundamentals of less stable ion−dipole complexes, such as those shown in Figure 1j−l. These may be formed in the ion source, for example, via three body association involving $C_6H_5^+$ and HF (both produced by fragmentation of $C_6H_6F^+$) or intracluster ion−molecule reactions of larger complexes, such as $C_6H_6F^+$−$(C_6H_5F)_n$−L_m (L = Ar, H$_2$, CH$_4$), with subsequent evaporative cooling. An alternative production pathway proceeds via isomerization of hot F-$C_6H_6F^+$ (produced by reaction 1). Subsequent collisional cooling below the interconversion barriers may prevent quantitative (back) isomerization of the less stable dimers toward F-$C_6H_6F^+$, the global minimum on the HF−$C_6H_5^+$ PES. Indeed, the calculated F−H stretch frequencies of all three HF−$C_6H_5^+$ isomers considered in Figure 1j−l (3895−3905 cm^{-1}) are close to the observed 3885 cm^{-1} band. A simulation of the IR spectrum of HF^{mo}−$C_6H_5^+$ is included in Figure 6. As the dissociation energies and IR spectra of HF^{pm}−$C_6H_5^+$ and HF$^{\pi}$−$C_6H_5^+$ are similar, the σ_{FH} fundamentals of several HF−$C_6H_5^+$ isomers may in fact contribute to the broad transition at 3885 cm^{-1}. If this assignment were correct, also part of the signal at 3125 cm^{-1} must originate from σ_{CH} of these HF−$C_6H_5^+$ isomers.

Clearly, the fluoronium ion of $C_6H_6F^+$ dominates the IR spectrum in Figure 6. The stick spectra calculated for the carbenium isomers reveal that the aliphatic C−H stretch vibration(s) of the (substituted) methylene group are their characteristic fingerprints in the investigated spectral range. These occur near 2600 and 2900 cm^{-1} for i-$C_6H_6F^+$ (CHF group) and the other carbenium ions (CH$_2$ group), respectively. Obviously, the experimental spectrum lacks absorptions in this range, implying that carbenium ions do not contribute to this spectrum. At first glance, this result may be surprising because the carbenium ions are more stable than F-$C_6H_6F^+$, and at least some of them (e.g., p,o-$C_6H_6F^+$) almost certainly occur with significant abundance in the $C_6H_6F^+$ beam under the present conditions.[17,25] However, overcoming the barrier for dehydrofluorination of cold carbenium isomers requires at least ~ 170 kJ/mol $\approx 14\ 200$ cm^{-1} (for i-$C_6H_6F^+$), corresponding to the absorption of more than four photons with $v_{IR} \approx 3000$ cm^{-1} (Figure 2). Apparently, the maximal available laser intensity (200 kW/cm^2) is insufficient to drive this multiphoton process. Resonant single photon dissociation of carbenium ions requires initial internal energies of > 130 kJ/mol. Evidently, the population of such energetic carbenium ions is below the detection limit when CH$_5^+$/C$_2$H$_5^+$ (mixture A) is used for protonation (section 4.1). This result is also consistent with the small MD signal in the mass spectra in Figure 5a. In contrast, using H$_3^+$/ArH$^+$ as protonating agent (mixture B), we found that a significant amount of carbenium ions with internal energies > 130 kJ/mol is produced,[28,29] as is signaled by the large $C_6H_5^+$ MD intensity in the mass spectra in Figure 5b. Efforts to record structured IR spectra of internally excited carbenium ions using mixture B, however, failed, mainly because of the large MD background.

Similar to the carbenium ions of $C_6H_6F^+$, the dissociation energy of F-$C_6H_6F^+$ may also be larger than the vibrational energies of the observed transitions. However, σ_{FH} and σ_{CH} of F-$C_6H_6F^+$ (3645 and 3125 cm^{-1}) are much closer to D_0 for F-$C_6H_6F^+$ than for the carbenium ions (D_0 > 11 000 cm^{-1}). Accurate experimental values for the ground-state binding energy of F-$C_6H_6F^+$ are not available, and thermochemical data yield an approximate enthalpy of 17 ± 25 kJ/mol (1420 ± 2090 cm^{-1}) for dehydrofluorination.[25,48] The D_0 value calculated at the MP2/6-31G* level is 41 kJ/mol (3430 cm^{-1}),[29] whereas the

(62) Nizkorodov, S. A.; Meuwly, M.; Maier, J. P.; Dopfer, O.; Bieske, E. J. *J. Chem. Phys.* **1998**, *108*, 8964.
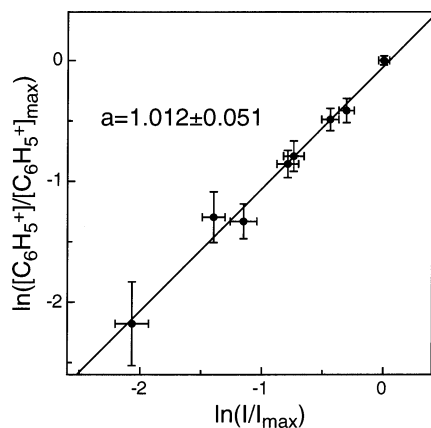(63) Ayotte, P.; Weddle, G. H.; Kim, J.; Johnson, M. A. *J. Am. Chem. Soc.* **1998**, *120*, 12361.

Figure 7. Double logarithmic plot of the normalized fragment yield, $[C_6H_5^+]/[C_6H_5^+]_{max}$, versus the normalized laser intensity, I/I_{max}, measured for the process described in eq 2 using $\nu_{IR} = 3645$ cm^{-1} (σ_{FH}). The straight line corresponds to a least-squares fit of the data to a first-order polynomial, and the derived slope of $a = 1.012 \pm 0.051$ indicates a one photon process.

higher B3LP/6-311G(2df,2pd) and MP2/6-311G(2df,2pd) levels yield $D_0 = 54$ and 51 kJ/mol (4521 and 4260 cm^{-1}), respectively. Thus, although available theoretical and experimental data are inconclusive as to whether D_0 of F-C$_6$H$_6$F$^+$ is below or above σ_{FH} and σ_{CH} (3645 and 3125 cm^{-1}), the high level calculations suggest that $D_0 > 4000$ cm^{-1}. Following this favored scenario, the experimental detection of σ_{FH} and σ_{CH} for F-C$_6$H$_6$F$^+$ must be explained either by two photon absorption of cold F-C$_6$H$_6$F$^+$ or by one photon absorption of complexes with internal vibrational energy prior to IR excitation ($E_{int} > 900$ and 1400 cm^{-1} for σ_{FH} and σ_{CH}, assuming $D_0 = 4521$ cm^{-1}). In the latter case, the C$_6$H$_5^+$ photofragment concentration, [C$_6$H$_5^+$], is proportional to $[1 - \exp(-\sigma I)]$, where σ is the cross section for single photon absorption, and I is the laser intensity.[64] For the low available laser intensity ($I_{max} = 200$ kW/cm^2), the relation can be approximated by $\ln([C_6H_5^+]/[C_6H_5^+]_{max}) = const + a \times \ln(I/I_{max})$ with $a = 1$. On the other hand, $a > 1$ is expected for two or more photon absorption of cold F-C$_6$H$_6$F$^+$. Figure 7 reproduces a double logarithmic plot of the normalized fragment yield versus the normalized laser intensity measured for σ_{FH} excitation (3645 cm^{-1}). The slope derived from a least-squares fit to a first-order polynomial, $a = 1.012 \pm 0.051$, suggests that the observed fragmentation signals arise (predominantly) from one photon absorption. Thus, the 3125 and 3645 cm^{-1} bands are attributed to $\sigma_{CH} + \nu_x \leftarrow \nu_x$ and $\sigma_{FH} + \nu_x \leftarrow \nu_x$ sequence transitions, which are regarded as good approximations of the σ_{CH} and σ_{FH} fundamentals. A similar situation occurs for the related H$_2$O$-$C$_6$H$_6^+$ complex investigated with the same setup.[47] The large widths of the transitions in the F-C$_6$H$_6$F$^+$ and H$_2$O$-$C$_6$H$_6^+$ spectra (20$-$45 cm^{-1}) are consistent with the observation of sequence transitions.

Assuming single photon absorption of relatively cold F-C$_6$H$_6$F$^+$ and a dissociation energy of $D_0 \approx 4500$ cm^{-1}, the (ro)vibrational excitation of the C$_6$H$_5^+$ and HF dissociation products in reaction 1 must be small. The HF fragment is in the vibrationless $^1\Sigma^+$ electronic ground state with low (or no) rotational excitation.

The C$_6$H$_5^+$ fragment is the phenyl cation in its ^{1}A$_1$ electronic ground state (with probably only minor vibrational excitation), as the lowest triplet state (^{3}B$_1$) and the most stable acyclic C$_6$H$_5^+$ isomers are at least $\sim$0.8$-$1 eV higher in energy.[65,66] Hence, IR photodissociation of F-C$_6$H$_6$F$^+$ does not induce ring opening. This observation is consistent with the narrow kinetic energy release (KER) component observed for F-C$_6$H$_6$F$^+$ in unimolecular decay studies using CH$_5^+$ as protonating agent.[17,29] An interesting question is whether photodissociation in F-C$_6$H$_6$F$^+$ is a mode-selective or a statistical process. For small and weakly bound complexes, often highly mode-selective dissociation dynamics is observed, whereas dissociation of larger and more strongly bound systems can usually be well described by statistical theories.[12,67−69] Unfortunately, the large widths of the transitions observed for F-C$_6$H$_6$F$^+$ are mainly arising from inhomogeneous broadening (hot band congestion) rather than from homogeneous broadening due to fast relaxation processes (intramolecular vibrational redistribution and/or predissociation). Consequently, the experimental spectrum does not allow one to decide which relaxation mechanism is faster in the present case.

5. Concluding Remarks

In summary, the fluoronium isomer of protonated fluorobenzene, F-C$_6$H$_6$F$^+$, is characterized by IR spectroscopy and quantum chemical calculations. The observed spectrum corresponds to the first structured spectrum of an isolated protonated aromatic molecule (AH$^+$) in the gas phase. Quantum chemical calculations of the C$_6$H$_6$F$^+$ PES reveal that ring protonation of C$_6$H$_5$F (carbenium ions, fluorobenzenium) is energetically preferred over F protonation (phenylfluoronium). Nonetheless, sufficient F-C$_6$H$_6$F$^+$ concentrations are produced using chemical ionization with CH$_4$ in a supersonic plasma expansion. The spectroscopic and theoretical data show that F-C$_6$H$_6$F$^+$ is best described as a HF$-$C$_6$H$_5^+$ ion$-$dipole complex. The dissociation energy for dehydrofluorination, that is, fragmentation into HF and cyclic C$_6$H$_5^+$ in their electronic ground states, is calculated to be only $D_0 = 4521$ cm^{-1} (54 kJ/mol) and enables the IR spectrum of F-C$_6$H$_6$F$^+$ to be observed by photodissociation. Under one photon absorption conditions, the F-C$_6$H$_6$F$^+$ isomer of C$_6$H$_6$F$^+$ can selectively be detected, whereas the more stable carbenium isomers do not contribute to the spectrum observed. The present experimental approach differs qualitatively from the previously used messenger technique to characterize AH$^+$ ions by IR photodissociation of their weakly bound AH$^+-$L$_n$ clusters using inert ligands L.[11,13] Although with the latter approach all AH$^+$ isomers produced in the ion source contribute to the observed spectrum, the properties of AH$^+$ are more or less modified by the weak microsolvation interaction with L.

The IR spectrum of F-C$_6$H$_6$F$^+$ confirms that protonation of C$_6$H$_5$F at the F atom strongly destabilizes the C$-$F bond and the charge of the added proton is mostly delocalized over the C$_6$H$_5^+$ ring (0.83 e). A similar destabilization of the usually extremely strong and inert C$-$F bonds in fluorocarbon molecules was reported for metal cations binding to the F atom.[21]

(64) In fact, the observed cross section corresponds to the product of absorption and dissociation cross sections. It is assumed that quantitative dissociation of metastable levels above the lowest dissociation limit can occur on the time scale of the experiment (that is, the flight time through the octopole). Thus, the observed cross section is proportional to the absorption cross section, as the dissociation cross section is roughly constant.

(65) Hrusak, J.; Schröder, D.; Iwata, S. *J. Chem. Phys.* **1997**, *106*, 7541.
(66) Lorquet, J. C.; Lorquet, A. J. *J. Phys. Chem. A* **2001**, *105*, 3719.
(67) Baer, T.; Hase, W. L. *Unimolecular Reaction Dynamics*; Oxford University Press: New York, 1996.
(68) Miller, R. E. *Science* **1988**, *240*, 447.
(69) Ewing, G. E. *J. Phys. Chem.* **1987**, *91*, 4662.

In line with the charge transfer, the geometry of F-$C_6H_6F^+$ is rather different from that of C_6H_5F, with the main effect that protonation leads to a compression of the ring. Moreover, comparison between σ_{FH} of F-$C_6H_6F^+$ and HFH^+ reveals that replacing H^+ by $C_6H_5^+$ stabilizes the F–H bond because of the charge delocalization in the $C_6H_5^+$ ring. In addition, the large difference in the dissociation energies of HF–H^+ ($D_0 \approx$ $PA_{HF} = 484$ kJ/mol)[30] and HF–$C_6H_5^+$ ($D_0 \approx 54$ kJ/mol) reflects the drastic effect upon substitution of H^+ by $C_6H_5^+$. Similar to cyclic $C_6H_5^+$, the closed shell CH_3^+ cation is a very electrophilic agent. Consequently, CH_3^+ forms a relatively strong bond even to the inert Ar atom ($-\Delta H_0 \approx 47 \pm 9$ kJ/mol) because of partial charge transfer from Ar to CH_3^+.[70,71] As a result, complexation of CH_3^+ with Ar has large structural effects similar to those of complexation of $C_6H_5^+$ with HF.

In conclusion, the fruitful combination of IR spectroscopy, mass spectrometry, and quantum chemistry is a powerful tool to determine the structure (in particular, the protonation sites) in AH^+ isolated in the gas phase and under controlled solvation conditions (e.g., AH^+–L_n).[11,13] Future efforts aim at the characterization of related reactive intermediates, such as other AH^+ ions and L–$C_6H_5^+$ complexes. Eventually, this strategy aims at the determination of the drastic effects of stepwise solvation on the properties of ion–molecule reaction mechanisms.

(70) Olkhov, R. V.; Nizkorodov, S. A.; Dopfer, O. *J. Chem. Phys.* **1998**, *108*, 10046.
(71) Hiraoka, K.; Kudaka, I.; Yamabe, S. *Chem. Phys. Lett.* **1991**, *178*, 103.